Extended Depth of Field for Fluorescence Microscopy

Julie Chang
EE 367
Stanford University
jchang10@stanford.edu

Abstract

High numerical aperture objectives result in extremely shallow depths of field, which may or may not be desired by the user of the microscope. When looking at extended objects, planes that arent necessarily perpendicular to the light path, or fluorophores that move in and out of focus, an extended depth of field (EDOF) would be useful to fully visualize the sample. PSF engineering can be applied to this problem with several advantages, including ease of implementation, no need for moving parts, and retention of high spatial frequencies. In this project, a cubic phase mask was used to achieve a depth-invariant PSF and acquire images with brightfield and fluorescence microscopy.

1. Introduction

Conventional microscopes image a two-dimensional cross-section of a three-dimensional sample in a single snapshot. Depth of field, essentially the thickness of this cross-section, measures the distance from the nearest object plane in focus to that of the farthest plane also simultaneously in focus. Depth of field for a microscope objective can be approximated by:

$$\text{DOF} = \frac{2\lambda_0 n}{\text{NA}^2}$$

where λ is the central wavelength of light passing through the system, n is the index of refraction of the medium between the sample and objective's front lens element, and NA is the objective's numerical aperture. For reference, a 40x objective with NA = 0.65 has a DOF of only around 1 μm.

High NA objectives are commonly used in fluorescence microscopy for their higher magnification power, resulting in shallow depths of field that can be frustrating to work with. When the structure of interest lies completely within the depth of field, there is no problem, and the structure is seen all in focus. However, when imaging extended objects or processes, it is difficult to capture the full information about the sample. Multiple images can be taken at different depths, but this process may be too slow to capture fast processes.

There are a number of methods that can be used to extend the native depth of field of a microscope. Perhaps the most obvious is to acquire a focal stack, i.e. to acquire images at multiple focal planes and then reconstruct a volume or flatten the frames into an all-in-focus image. A focal sweep translates the image sensor or objective during a single exposure and then relies on post-processing to deblur the image. A ring-shaped annulus can be placed at the pupil plane aperture to generate a Bessel-like beam, which generates extends the depth of field since Bessel beams are theoretically non-diffracting [1].

The approach of this project is to achieve a depth invariant PSF with a cubic phase mask (CPM). A depth invariant PSF means that objects at any depth are convolved with the same blur kernel to product the output image. Hence, deconvolution with a single known PSF could potentially restore features at all depths. This is relatively convenient to implement, since it involves only the addition of a phase plate at the back aperture of the objective or any of its conjugate planes. After that, there will be no moving parts during imaging, giving it an advantage over the focal stack and focal sweep techniques. There is no need for a long scan time, allowing for high-speed imaging. A phase mask, unlike an amplitude mask, affects only the phase of the incoming wavefront, which maximizes optical power arriving at the image plane.

2. Wavefront coding via cubic phase mask

Wavefront coding was first popularized in computational photography and generally refers to the use of a phase modulating element in image acquisition followed with deconvolution to restore image quality over an extended depth of field. There are many varieties of phase masks, including cubic, sinusoidal, and axicon-based [2]. For this project a cubic model was chosen because it is the most widely used and a CPM was readily available. Experimentally, CPM imaging systems have demonstrated an increase of 10 times

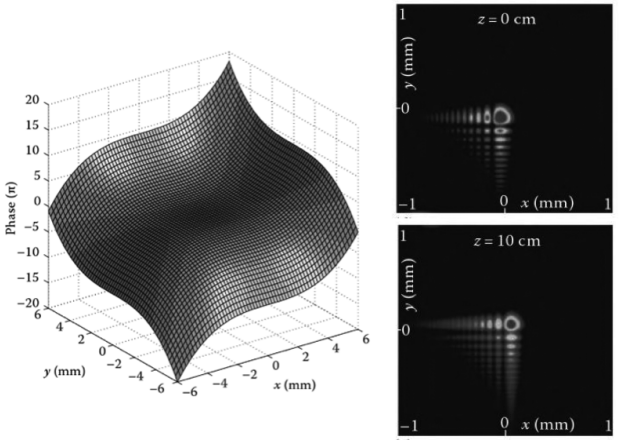

Figure 1. Cubic phase mask model and corresponding PSFs at plane of best focus and 10 cm out of focus. Figure adapted from from [1].

the depth of focus of standard systems [3]. The goal of this project was to set up and evaluate EDOF with a CPM for fluorescence microscopy, and potentially extend it to other applications in the future.

The use of a CPM was pioneered by Dowski and Cathey around 20 years ago [4]. Their design of an EDOF system leads to a CPM solution with thickness corresponding to this 2D spatial function:

$$P(x, y) = a(x^3 + y^3)$$

The phase delay caused by the mask is then

$$\phi(x, y) = \text{mod}(\alpha(x^3 + y^3), 2\pi)$$

where a and α are related by the index of refraction of the material and the wavelength of light. The complex transmission function, also referred to as the optical transfer function (OTF), is given by

$$H(x, y) = \exp\left(i\phi(x, y)\right)$$

The point spread function (PSF) is defined as the Fourier transform of the OTF. An example of a CPM and PSFs at best focus and at a plane of misfocus are shown in Figure 1. The shapes of the two PSFs are similar, but the center of the largest peak shifts with misfocus. The α parameter can be increased to minimize the sensitivity of the CPM system to movement of the PSF with misfocus, though at the expense of the image's signal intensity.

3. Simulations

A cubic phase mask was simulated with $\alpha = 8\pi$ to include about 7-8 phase cycles from the diagonal . The corresponding PSF at best focus is shown in Figure 2. The CPM

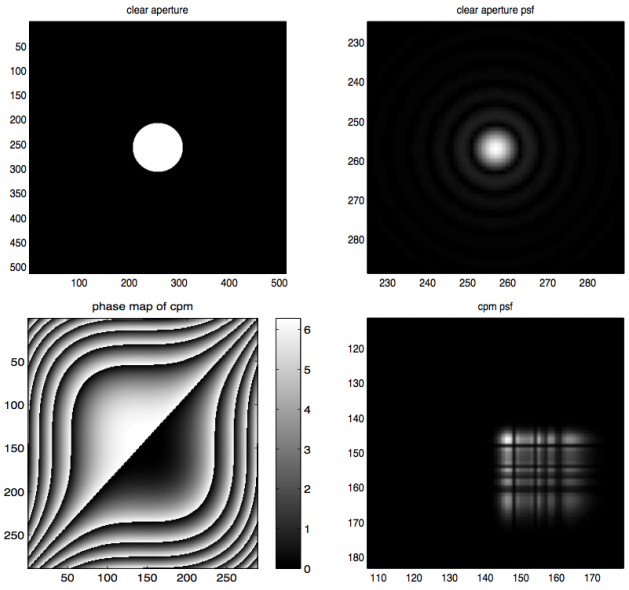

Figure 2. Clear aperture vs. cubic phase mask.

PSF is markedly different from the typical PSF formed from a clear aperture. The phantom object for simulations was a chirped resolution target repeated in a 3x3 matrix. The relative intensity of the charts decreases from left to right (1.00, 0.75, 0.50), and the distance from best focus increases from top to bottom. In Figure 3, (a) simulates the blurring induced by a clear aperture objective without noise and (b) shows the blurred EDOF image with Gaussian noise added. The result of Wiener filtering with the modeled PSF is shown in (c). After deconvolution, features in all three rows can be resolved, though there are still remnants of the CPM PSF and noise. In addition, Wiener filtering tends to introduce ringing artifacts into the image. ADMM or other deconvolution techniques have the potential for better image restoration.

4. Experimental

4.1. Microscope Setup

The setup used is shown in Figure 4. Samples are imaged with a commercial Olympus microscope capable of bright-field and epi-illumination. Two f = 200 mm lenses form a 4F system after the microscopes image plane to provide easy access to a conjugate plane of the back focal plane. A CPM from RPC photonics was mounted in a rotational mount connected to a translational mount and placed at the Fourier plane between the lenses. The stand could be easily removed from the optical path to allow for comparison with and without the CPM. All optical elements were aligned with a laser alignment tool that could be screwed

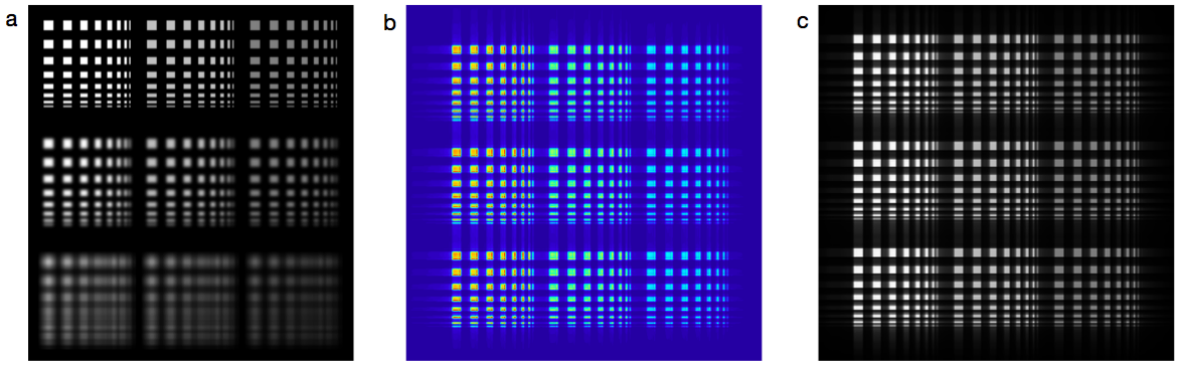

Figure 3. Simulated stepped resolution chart. (a) simulates the blurring induced by a clear aperture objective absent noise. (b) simulates the blurred and noisy EDF. (c) shows the results of Wiener filtering with the model CPM PSF.

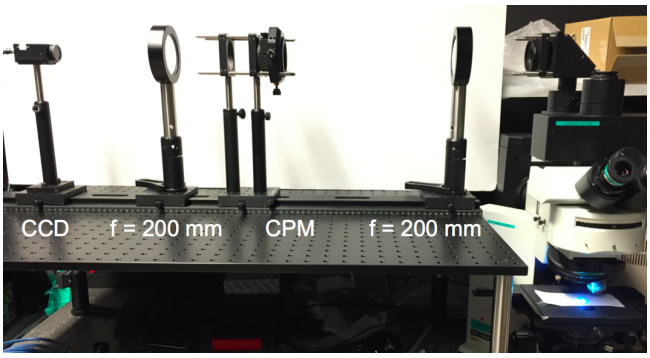

Figure 4. Microscope setup. Cubic phase mask is placed at the Fourier plane of a 4F system that extends from a camera port of a commercial Olympus microscope.

into an objective ring. Images were captured with a Point-Grey Grasshopper 3 CCD camera.

The PSFs produced by this microscope setup from a 5 μm pinhole are shown in Figure 5. The typical PSF from a clear aperture (CA) at the focal plane is pictured in (a). Examples of CPM PSFs are shown in (b-d). The shape matches those from literature and the model, but the peak intensity is much lower than that of the CA PSF. The CPM PSFs are relatively invariant from -30 μm to +30 μm from the plane of best focus. By $\pm$50 μm (Fig. 5d), the CPM PSF is significantly different.

4.2. Results

First, brightfield illumination was used to image a 1951 USAF resolution test chart. After finding the plane of best focus, the stage was moved up and down to observe the effect of misfocus. When the CPM was in place, the plane of best focus was blurred, but high resolution could be restored with deconvolution using the experimentally captured PSF (Fig. 5b). The distinct PSF pattern produced by the CPM could be seen in the unprocessed images. Of more interest was the comparison between CA and CPM images at misfocus. Figure 6(b-d) show the test chart 30 μm above the plane of best focus without the CPM, with the CPM and after deconvolution with Wiener filtering. In (d), some of the sharp edges have been restored, and the image SNR is improved.

Next epi-illumination with blue light was used to image a sample of .2 μm diameter yellow-green fluorescent beads (Invitrogen) in 1% agarose. Fluorescence was observed using a 20x objective. Figure 6(e-f), images without the CPM focused at different depths within the sample, are included to demonstrate the impossibility of capturing the entirety of an extended sample in one image. The bottom row of Figure 6 shows images of the same sample with the CPM in place (h), after deconvolution with ADMM (i), and Wiener filtering (j). The image processing here did not clearly restore the sample features. This is likely due to an inaccurate PSF used for deconvolution. The sample of beads was too concentrated and the image on the camera too noisy to capture a reliable PSF from a single bead, so the CPM PSF from Figure 5 was used instead.

5. Discussion

There are many adjustments that still need to be made to this system to improve final image quality. First, alignment of the multiple adjustable parts of the setup could be more finely tuned. Alternatively, phase masks are more commonly placed within the body of the microscope, between the objective and tube lens, avoiding the need for the extra pair of relay lenses used here. This option has advantages of a more compact design as well as fewer parts for alignment. A more accurate PSF would allow for more reliable deconvolution. A camera with higher sensitivity and lower noise could capture a clearer PSF, or the CPM's specs could allow

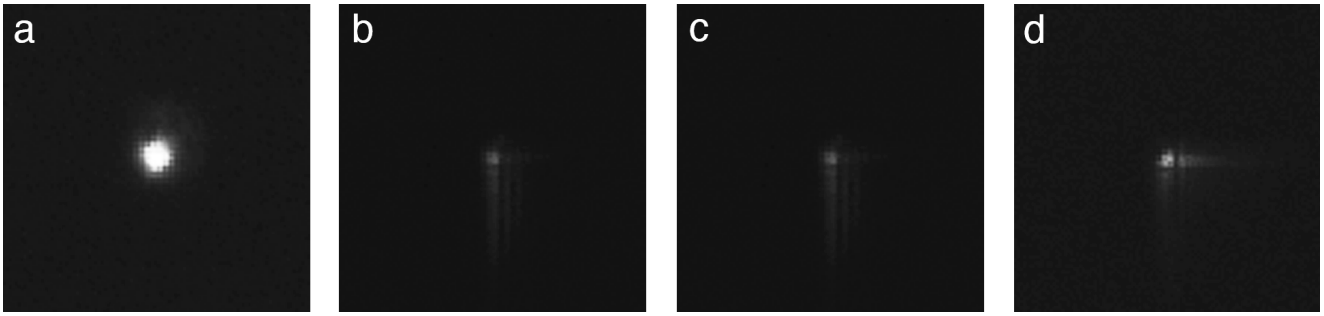

Figure 5. Point spread functions captured from a 5 μm pinhole placed on the microscope stage. Images show the relative shapes and intensities of the PSFs without the CPM (a) and with the CPM at best focus (b), 30 μm above focus (c), and 50 μm above focus (c).

for a precise modeling of the PSF. Finally, deconvolution algorithms can be explored in more detail to identify the best option in terms of SNR, MSE (for simulated images), and image artifacts.

There are several applications for EDOF in biology, besides just for use on its own. Wavefront coding could be combined with light sheet microscopy to increase imaging speeds, since the sample or objectives would no longer need to be moved to adjust the focal plane. Instead, the light sheet could be swept through the sample quickly and images could be processed after acquisition. EDOF is also potentially useful for the imaging setup in microfluidic systems, preventing the monitoring system from missing or incorrectly categorizing a particle, droplet, cell, etc. just because it was slightly out of focus. This could be especially important when the target for detection is extremely rare.

Acknowledgments

Thanks to Gordon Wetzstein for instructing EE 367 and guiding this course project. I would also like to thank Isaac Kauvar and Samuel Yang for providing advice as well as the CPM and miscellaneous parts for the microscope.

References

[1] Wicker, K. and Heintzmann, R. "Chapter 4. Fluorescence microscopy with extended depth of field." *Nanoscopy and Multidimensional Optical Fluorescence Microscopy.* ed. Alberto Diaspro. 2010.

[2] Zahreddine, R. and Cogswell, C. "Total variation regularized deconvolution of Poisson noise dominated extended depth of field images". *Applied Optics*. 2015.

[3] Zhao, T., Mauger, T., and Li, G. "Optimization of wavefront-coded infinity-corrected microscope systems with extended depth of field." *Biomedical Optics Express*. 2013.

[4] Dowski, E. and Cathey, T. "Extended depth of field through wave-front coding." *Applied Optics*. 1995.

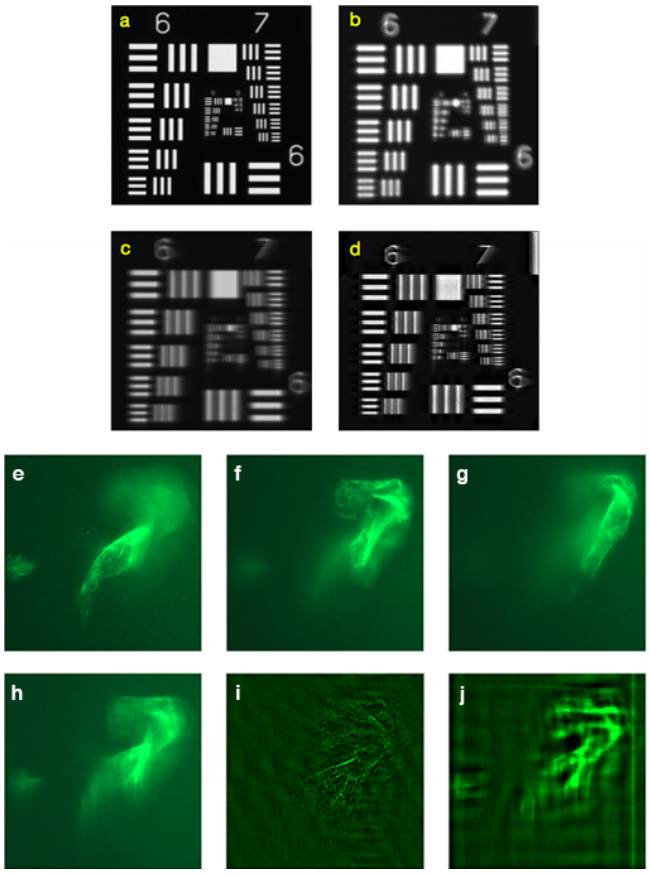

Figure 6. Sample images using brightfield (a-d) fluorescence (e-j) microscopy. USAF resolution test chart imaged with 10x objective (a) in focus without CPM, (b) 30 m out of focus, (c) 30 μm out of focus with CPM, and (d) 30 μm out of focus with CPM after deconvolution with experimentally captured CPM PSF. (e-f) show images of .2 μm diameter fluorescent beads in 1% agarose using a 20x objective, illuminated with blue light, captured without CPM at different focal planes. The bottom row shows the blurred image using the CPM (h) and after deconvolution with ADMM (i) and Wiener filtering (j).